Continuous Shared Control for Stabilizing Reaching and Grasping With Brain-Machine Interfaces

Hyun K. Kim* , S. James Biggs, *Member, IEEE*, David W. Schloerb, Jose M. Carmena, *Member, IEEE*, Mikhail A. Lebedev, Miguel A. L. Nicolelis, and Mandayam A. Srinivasan

***Abstract*—Research on brain-machine interfaces (BMI's) is directed toward enabling paralyzed individuals to manipulate their environment through slave robots. Even for able-bodied individuals, using a robot to reach and grasp objects in unstructured environments can be a difficult telemanipulation task. Controlling the slave directly with neural signals instead of a hand-master adds further challenges, such as uncertainty about the intended trajectory coupled with a low update rate for the command signal. To address these challenges, a continuous shared control (CSC) paradigm is introduced for BMI where robot sensors produce reflex-like reactions to augment brain-controlled trajectories. To test the merits of this approach, CSC was implemented on a 3-degree-of-freedom robot with a gripper bearing three co-located range sensors. The robot was commanded to follow eighty-three reach-and-grasp trajectories estimated previously from the outputs of a population of neurons recorded from the brain of a monkey. Five different levels of sensor-based reflexes were tested. Weighting brain commands 70% and sensor commands 30% produced the best task performance, better than brain signals alone by more than seven-fold. Such a marked performance improvement in this test case suggests that some level of machine autonomy will be an important component of successful BMI systems in general.**

***Index Terms*—Brain-machine interface, neuroprosthesis, shared control, telerobotics.**

I. INTRODUCTION

WITH advances in measuring and decoding the electrical activity of large populations of single cortical neurons it is gradually becoming practical to control robot limbs with brain signals. In the first demonstration of such a brain machine interface (BMI) based on the individual outputs of a large population (>50 units) of cortical neurons [1], the feasibility of 3-*degree-of freedom* (DOF) robot teleoperation over the Internet was established. Recently, Carmena *et al.*, [2] demonstrated how rhesus monkeys (Macaca mulatta) were able to control a robot arm using visual feedback (Fig. 1). Neural signals recorded from multiple cortical areas were fed through a computational fitting algorithm (Wiener filter) that decoded hand position, velocity, and grasping force information during reaching and grasping tasks. Movement parameters predicted by the algorithm drove the robot arm to match the monkey's intentions. Under the same BMI paradigm, other groups have reported brain control displacement of computer cursors [3], [4].

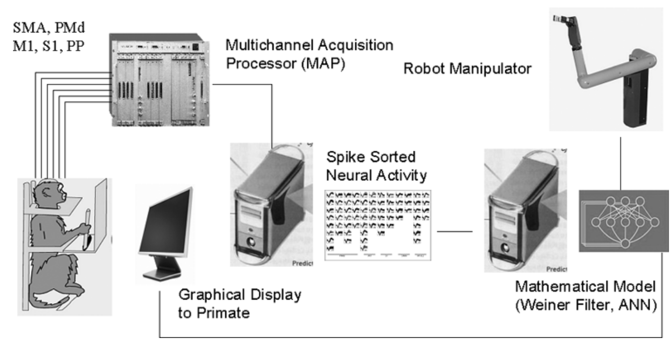

Fig. 1. System diagram form BMI setup reported in Carmena *et al.*, [2].

From a manipulator control standpoint, BMI presents unique challenges to both the roboticist and user. The following sections describe these challenges, as well as a continuous shared control (CSC) paradigm designed to overcome some of them.

A. Challenges of Brain Machine Interface

Uncertainty in determining the command signal presents one of the main difficulties in agile control of a BMI robot. A probable source of this uncertainty is the sparse sampling of the population of cortical neurons. Current microwire arrays allow for recording of approximately 10^2 neurons, an order of magnitude better than was possible until very recently, but still a miniscule fraction of the approximately 10^{11} neurons in the brain. Placing the microwire arrays in brain areas known to be related to motor control obviously improves the performance, but the undersampling problem seems likely to remain an aspect of BMI systems for some time. This undersampling is partially offset by redundancy in motor information in the neuron firings. However, this redundancy is limited, and does not provide assurance that all the relevant information is present in the neurons that are being recorded. Even in arm motor and premotor areas, it appears that only a relatively small portion of cortical neurons are involved with direct encoding of movement features. Studies show large

Manuscript received May 28, 2004; revised July 17, 2005. This work was supported in part by the Defense Advanced Research Projects Agency (DARPA) under Grant N66001-02-C-8022, and by the Christopher Reeve Paralysis Foundation, which supported JMC. *Asterisk indicates corresponding author.*

*H. K. Kim is with the Touch Laboratory, Massachusetts Institute of Technology, 50 Vasser Street, Room 36-789, Cambridge, MA 02139 USA (e-mail: hyunkim@mit.edu).

S. J. Biggs, D. W. Schloerb, and M. A. Srinivasan are with the Touch Laboratory, Massachusetts Institute of Technology, Cambridge, MA 02139 USA (e-mail: jbiggs@mit.edu; schloerb@mit.edu; srini@mit.edu).

J. M. Carmena is with the Department of Electrical Engineering and Computer Sciences, and Helen Wills Neuroscience Institute, University of California, Berkeley, CA 94720 USA (e-mail: carmena@eecs.berkeley.edu).

M. A. Lebedev and M. A. L. Nicolelis are with the Department of Neurobiology and Center for NeuroEngineering, Duke University Medical Center, Durham, NC 27710 USA (e-mail: lebedev@neuro.duke.edu; nicoleli@neuro.duke.edu).

Digital Object Identifier 10.1109/TBME.2006.870235

portions of the neurons are correlated to more abstract characteristics such as potential targets, position of obstacles and orientation of spatial attention [5]–[7].

Due to limited understanding of the information represented by neuronal discharges and the sparse sampling, no model can reconstruct exactly the intended motion from the neural activity recorded. Current microelectrode arrays gather enough data to predict two-dimensional or three-dimensional hand coordinates with an average correlation coefficient (r^2) of about 0.65–0.8. If position is predicted, the decoded output resembles the monkey's arm trajectory with noise added. The unsteadiness of the output trajectory makes dexterous manipulation very difficult. Although a low pass filter may be used to reject some of the noise, such a filter results in a delayed response and loss of the ability to make quick movements.

The frequency of the decoded command signals can also present problems. In algorithms used in current BMI systems, cortical activity is commonly binned and processed at 10–20 samples/s, for optimal prediction. This works adequately for positioning a robot limb in free space, or moving a cursor on a computer monitor. However, this is a very low update frequency for commanding a slave robot interacting with real objects. Purposeful human movements range from approximately 0.01 Hz (posture) to about 10 Hz (physiologic tremor) [8]. To command a robot limb over this range of frequencies requires updates of at least 20 samples/s to meet the Nyquist criterion, or 200 samples/s in order to have 10 samples/half-cycle. The neural recordings can be binned more frequently than the typical 10–20 cycles/s. However, doing so may affect the accuracy of the prediction, may increase the noise in the predicted signals, and may require more computational power than current processors can provide.

Dexterous manipulation is further complicated by the lack of tactile feedback. Numerous teleoperation studies have shown that force feedback can improve performance dramatically [9], [10]. Unless the interface stimulates somatosensory cortex by passing small currents through electrodes, or the skin with tactile stimulation, the robot and gripper are insensate to the BMI user. Key problems of an insensate gripper are damage and delicacy. A user who does not feel pain when a slave gripper collides roughly with an object may damage the gripper mechanism or sensors by accident (humans) or indifference (monkeys). Furthermore, delicate grasping of fragile objects usually requires sensing of grip force [11] and incipient slip [12].

B. Continuous Shared Control

Despite the difficulties just outlined, the BMI user needs dexterous manipulation of the robot in unstructured environments. To meet this challenge, a new control paradigm is proposed where the control is shared between the command signals from the user's brain and reactive signals from local sensors. This control paradigm can be described as one of *continuous shared control*. While the command signal from the user retains continuous control of the end position, the robot also reacts to local sensors detecting proximity, collisions or other relevant information.

The idea of control shared between sensors and high-level command signals has a long history. Salisbury [13] originally proposed a control strategy for a robotic hand, where the human can intervene in the autonomous task executed by the robot and, conversely, the robot can augment direct commands issued by the operator. Hayati and Venkataraman [14] presented a strategy detailing a framework for task level sharing of motion trajectories between the sensors and user. Since then, shared control has been used for numerous applications where disability of the user makes the command signal unreliable, where the environment is unpredictable and where the task is too difficult for direct teleoperation, or a combination of these factors. Examples of applications can be seen in navigation of wheel chairs and walkers [15], [16], trajectory control of satellites [17], and, most widely, for dexterous manipulation in teleoperation [9], [18]–[25]. Although the idea of shared control is not new, the present study is, to the authors' knowledge, the first application of shared control to Brain Machine Interfaces.

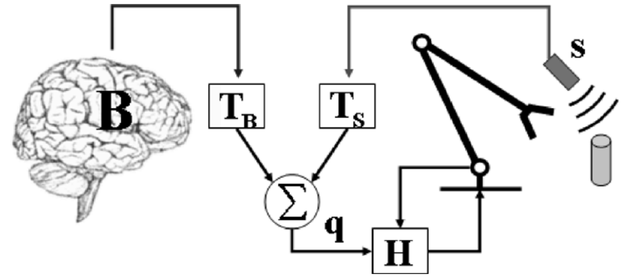

Fig. 2. The general problem of shared control in brain machine interfaces. The goal is to share control between commands arising from the user's brain $(\mathbf{B})$ and sensors $(\mathbf{S})$ on the slave device in a way that improves task performance. Both types of signals must be transformed (e.g., by $\mathbf{T_B}$, $\mathbf{T_S}$) into a "normal" command (e.g., a set of joint angles $\mathbf{q}$) on which a control system $(\mathbf{H})$ may operate.

C. Design of the Shared Control System

The authors have found the phrase "continuous shared control" useful for distinguishing the particular form of control implemented in this study from the range of possible BMI control schemes. First, the control is *continuous* because the interaction is immediate and does not have the "wait and see" characteristics of a planner-based approach or the switching characteristic of a traded-control [14]. The control is *shared* because it always reflects input of both brain and sensor, again distinguished from traded control where control switches discreetly from direct operator control to the autonomy of the robot depending on task and situation (Fig. 2).

As in prior studies, the CSC system makes the robot's reaction to the environment partially dependent on a mapping from a sensor set to an associated action-based set of rules, in a purely reactive fashion (versus planner-based). This is similar to what might be found in the zeroth layer of the subsumption architecture presented by Brooks [26]. Such reflexive actions have been previously incorporated in grasp execution of Turki and Coiffet's robot hand [21], the Utah/MIT dexterous hand [19] and NASA's Robonaut humanoids hand [24]. In these cases, dexterous and delicate grasping of objects, that would otherwise be impossible, is achieved through force sensing and visual servoing.

Although reflexive reactions have been used previously to stabilize grasping with general-purpose robots, it is worth noting the special importance of sensor-based reactions to BMI's. Sensor-based reactions added to a BMI system do more than merely improve the behavior of the robot. Rather, they can be viewed as a component necessary to *replace* the function of missing spinal and cerebellar reflexes that would normally facilitate manipulation. Muscle activity due to reflexes of the cerebellum and spinal cord or due to passive mechanical properties of the muscles are not reflected in the cortical electrodes of BMI at all or not until much after the activity has taken place. Therefore, for the system to approach normal human limb performance, it should be necessary to substitute for these reflexes in hardware and software. Accordingly, it is reasonable to choose control laws for sensor-based reactions that directly mimic or at least functionally replace biological motor reflexes.

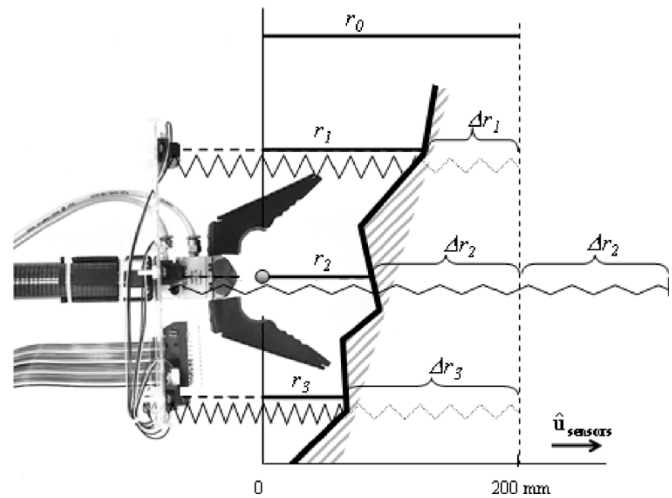

Fig. 3. Trials were conducted with a pneumatic gripper mounted on a backdriveable robot. Three triangulating infrared proximity sensors are mounted at the gripper base. The centroid of the sweet spot of the gripper is shown (ball), along with portions of the gripper that contacted a target object when it was grasped in the sweet spot (semicircular recesses in gripper jaws). The sweet spot was the location that results in the most stable grasp of the target object. The lines of sight of the sensors are shown (dashes aligned with $\hat{\mathbf{u}}_{\mathbf{sensors}}$). Range readings $(r_1, \ldots, r_3)$ from a simulated surface illustrate terms in (2) and (6). Cartoon springs displaced from rest (dashes up to r_0) illustrate how the sensor control laws embodied in (2) and (6) repelled the gripper from surfaces in front of flanking sensors (r_1 and r_3) and attracted it to surfaces in front of the central sensor (r_2).

II. Method

CSC was implemented in a robotic manipulator with proximity sensors in order to replace grasping functionality normally provided by two reflex reactions in biological organizms. The first reaction was a collision avoidance reflex roughly analogous to "pain withdrawal" [33]. This reflex withdrew the robot when either of the sensors just outside the outer edges of the gripper detected the presence of an obstacle, or impending inappropriate contact with the target. The second reflex replaced the functionality of the "infant palmar grasp reflex" [34]. When the sensor viewing the space within the span of the gripper detected an object, it attracted the robot toward it and biased the gripper toward closing. Engineering tests and a grasping task experiment, which used previously recorded brain-commanded trajectories, were then performed with the system.

A. Hardware—Proximity Sensors Co-Located With Gripper

Previous studies on shared control in teleoperation have shown that local sensors are most useful in obstacle avoidance and accurate grasping. Accordingly, the implementation of the CSC paradigm presented in this paper uses proximity sensors co-located with a robot gripper in order to provide obstacle avoidance and stabilized grasping. Fig. 3 shows the three triangulating infrared proximity sensors (Sharp GP2D120 Infrared Ranger, Acroname Inc., Boulder CO) attached to the base of a pneumatic gripper (Festo, HGR-10-A) mounted on a robot (Phantom 3.0, Sensable Technologies, Woburn MA).

The design of the location and action of the sensors in this study was deliberately biomimetic. Sensors were chosen that could report range of an object near the gripper much like the antennae of an ant or the vibrissae of a rat report range of an object near the animal's mouth. A variety of sensors mounted at a variety of positions could have reported the same information. Ultrasound, scanned laser, stereovision, and a co-located monocular camera system [27] were all considered. Co-located 1-DOF optical range sensors were chosen for several reasons.

Co-location was chosen because it seemed anatomically correct. Many animals that grasp with the mouth have vibrissae or antennae situated near it. Even animals with prehensile limbs, such as primates, rely highly on co-located tactile feedback from the finger pads for dexterous grasping. Co-location of the sensor also avoided potential problems of an obstruction lying between the sensor and target.

Optical sensing was chosen for cost-effectiveness, robustness, and lightness. Moreover, these specific optical range sensors were selected for their low computational expense compared to more complicated machine vision systems. Machine vision and visual servoing are well-established fields where the basic paradigms have largely been defined [28]–[30]. In a typical vision-based robotic grasping system stereo cameras are used to determine the position and the orientation of the object. In many cases a three-dimensional (3-D) model of the object is generated to visually track the target object. The same 3-D model is used for model-based simulations to plan the grasp and movement trajectories. During the execution, the visual system also monitors task execution. The system usually requires substantial computational power for processing the information and a "wait-see" approach during the planning stage. In the present BMI application, low computational overhead was required in order to maintain the relatively high servo rate (1000 Hz) required by the backdrivable robot (Phantom 3.0). The three infrared range sensors required far less data processing than a scan of every point in a 3-D scene would have. The simplicity of the computation was in tune with that of a biological reflex loop. In reflex actions, the responses are immediate and uncomplicated and vibrissae and antennae serve as simple range sensors much like the infrared sensors used.

B. Software—Shared Control With Sensor Readings Driving Simulated Reflexes

A reasonable, general-purpose paradigm for CSC can be introduced in the form of the artificial field potentials described by Khatib [31]. In this paradigm the robot moves in a field of forces. In the BMI CSC version of this concept, the brain-derived field U_{brain} has an attractive pole at the Cartesian coordinates estimated to be the desired gripper location. When one or more sensors collocated with the gripper detects the proximity of an object, it causes a sensor-based field potential, U_{sensors}, which may have local attractive or repulsive regions depending on the control laws of the individual sensors. The field potential for the gripper moving under shared control is the sum these two fields (1)

$$U_{\text{shared}} = U_{\text{sensors}} + U_{\text{brain}} \tag{1}$$

The only constraint on U_{sensors} is that the system be asymptotically stable. Thus, the design space for U_{sensors} is large and depends on the desired reflex response for the task and environment. For the implementation shown in this paper, a simple and effective quadratic potential field function was chosen. It treated range information from the sensors $(r_1, \ldots, r_3)$ as displacements of linear springs (Fig. 3) from rest (r_0)

$$U_{\text{sensors}} = \frac{1}{2} K_s \left[\left(\Delta r_1^+\right)^2 - \left(\Delta r_2^+\right)^2 + \left(\Delta r_3^+\right)^2 \right] \tag{2}$$

where the following hold.

Δr^+	$\max[\Delta r, 0]$.
Δr_i	$r_0 - r_i$.
r_1	calibrated range reading from left flanking sensor (in millimeters).
r_2	calibrated range reading from central sensor (in millimeters).
r_3	calibrated range reading from right flanking sensor (in millimeters).
r_0	range corresponding to rest length of virtual springs (in millimeters).
K_s	spring constant.

The negative sign of Δr_2 produced a linear spring-like attraction toward objects within the span of the gripper, in the line-of-sight of sensor r_2. This attraction facilitated task performance by advancing the gripper toward graspable objects. Conversely, the positive signs of Δr_1 and Δr_3 gave the gripper a linear spring-like repulsion away from objects just outside the gripper span, in the lines-of-sight of the flanking left and right sensors r_1 and r_3. This repulsion facilitated task performance by withdrawing the gripper from objects with which the outer gripper surface was about to collide. The resulting potential field for U_{sensors} with a target object is shown in Fig. 4.

The field potential U_{brain} for control of the brain-derived trajectory was straightforward. In online trials, binned neural signals were processed through a Wiener filter, as detailed elsewhere [2], in order to compute a brain-derived estimate of the correct gripper coordinates $\mathbf{x_{brain}}$. In the offline experiments on CSC reported here, the inverse kinematics of the robot were solved for the corresponding set of joint angles, $\mathbf{q_{brain}}$. The choice of proportional-derivative control in joint angle space gave the brain-derived potential field U_{brain} the following form in joint-angle space:

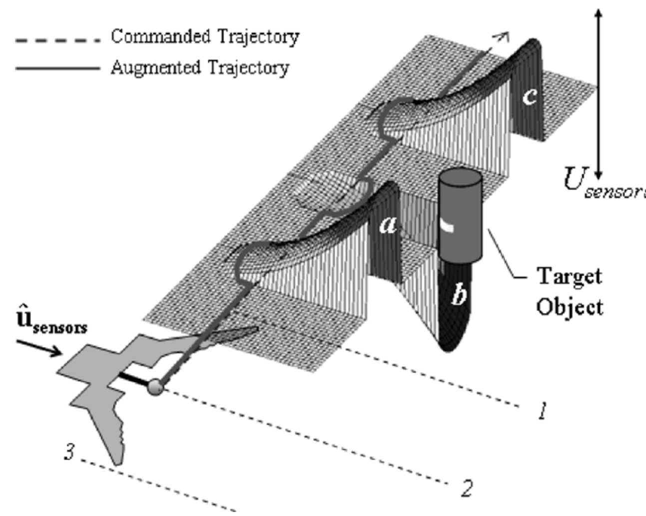

Fig. 4. Artificial potential field introduced by the sensor reflexes. Without shared control, the robot would move the gripper sweet spot (indicated by the ball on line "2") along the brain-commanded trajectory. With shared control, the combination of sensors and target causes a potential field that produces an augmented trajectory. As the gripper progresses, sensor 1 scans the target object, creating the nearest repulsive potential (a), which urges the gripper "downhill" in the direction $-\hat{\mathbf{u}}_{\mathbf{sensors}}$. With adequate gain, this effect prevents collisions between the gripper and target object. When sensor 2 scans the target object, the central attractive region (b) is produced, urging the gripper "downhill" toward the object, in the direction $+\hat{\mathbf{u}}_{\mathbf{sensors}}$. Sensor 3 produces the most distant repulsive field (c).

$$U_{\text{brain}} = \frac{1}{2} K_p (\mathbf{q} - \mathbf{q_{brain}})^2 + \frac{1}{2} K_d (\dot{\mathbf{q}} - \dot{\mathbf{q}}_{\mathbf{brain}})^2 \tag{3}$$

where the following hold.

U_{brain}	field potential derived from brain signals.
$\mathbf{q}$	joint angle encoder readings of the robot.
$\mathbf{q_{brain}}$	brain derived estimate of the correct joint angles.
$\dot{\mathbf{q}}$	$[\mathbf{q}(t) - \mathbf{q}(t - \Delta t)]/\Delta t$.
$\dot{\mathbf{q}}_{\mathbf{brain}}$	$(\mathbf{q_{brain}}(t) - \mathbf{q_{brain}}(t - \Delta t))/\Delta t$.
K_p	Gain of proportional control.
K_d	Gain of derivative control.

Solving Lagrange's equations for the energy functions resulted in the following implementation of the control ((4)–(8)). The motor torques of the robot, decoupled from dynamic terms, were a weighted sum of commands coming from two sources: 1) sensors on the slave robot; 2) the user's brain signals

$$\boldsymbol{\tau}_{\mathbf{shared}} = \boldsymbol{\tau}_{\mathbf{sensors}} + \boldsymbol{\tau}_{\mathbf{brain}}. \tag{4}$$

The first set of torques in (4), ($\boldsymbol{\tau}_{\mathbf{sensors}}$), were those derived from sensor readings. When no object was in the line of sight of the sensors, these torques were zero. However, when objects were present, the sensor-based potential field U_{sensors} became sloped, and the local gradient in the sensor-derived potential field (2) was equivalent to a virtual spring force $\mathbf{F}_{\mathbf{sensors}}$ acting on the gripper

$$\mathbf{F}_{\mathbf{sensors}} = \nabla[U_{\text{sensors}}]. \tag{5}$$

This virtual force had a magnitude, (F_{sensors}), equal to the sum of three spring forces with potential energy defined previously in (2). For any given set of sensor readings $\{r_1, r_2, r_3\}$, the virtual force acting on the gripper was

$$F_{\text{sensors}} = -\frac{1}{2}K_s\left[\left(\Delta r_1^{+}\right) - \left(\Delta r_2^{+}\right) + \left(\Delta r_3^{+}\right)\right]. \tag{6}$$

This virtual force acted in a direction aligned with the sensors lines-of-sight ($\hat{\mathbf{u}}_{\mathbf{sensors}}$), and produced torques about the robot joints ($\boldsymbol{\tau}_{\mathbf{sensors}}$) determined by the transpose of the robot Jacobian ($\mathbf{J}^{\mathbf{T}}$)

$$\boldsymbol{\tau}_{\mathbf{sensors}} = F_{\text{sensors}}\mathbf{J}^{\mathbf{T}}\hat{\mathbf{u}}_{\mathbf{sensors}}. \tag{7}$$

The second torque term in (4), ($\boldsymbol{\tau}_{\mathbf{brain}}$), was proportional-derivative control that urged the robot joints toward the brain-derived pose ($\mathbf{q}_{\mathbf{brain}}$). Since the potential field U_{brain} associated with this command was expressed in joint coordinates (3), the form of the potential gradient was simple. Using variables previously defined in (3), it had the form

$$\boldsymbol{\tau}_{\mathbf{brain}} = K_p(\mathbf{q} - \mathbf{q}_{\mathbf{brain}}) + K_d(\dot{\mathbf{q}} - \dot{\mathbf{q}}_{\mathbf{brain}}). \tag{8}$$

Finally, nonlinear control components were added to $\boldsymbol{\tau}_{\mathbf{shared}}$ to compensate for the dynamic and gravitational forces of the manipulator

$$\boldsymbol{\tau} = \boldsymbol{\tau}_{\mathbf{shared}} + \mathbf{H}(\mathbf{q})\ddot{\mathbf{q}}_{\mathbf{r}} + \mathbf{C}(\dot{\mathbf{q}}, \mathbf{q})\dot{\mathbf{q}}_{\mathbf{r}} + \mathbf{g}(\mathbf{q}). \tag{9}$$

The three dynamic terms include inertial torques, $\mathbf{H}(\mathbf{q})\ddot{\mathbf{q}}_{\mathbf{r}}$, Coriolis and centrifugal torques, $\mathbf{C}(\dot{\mathbf{q}}, \mathbf{q})\dot{\mathbf{q}}_{\mathbf{r}}$, and gravitational torques, $\mathbf{g}(\mathbf{q})$, where $\ddot{\mathbf{q}}_{\mathbf{r}}$ and $\dot{\mathbf{q}}_{\mathbf{r}}$ are the referenced joint accelerations and velocities, respectively [32]. The variables $\ddot{\mathbf{q}}_{\mathbf{r}}$ and $\dot{\mathbf{q}}_{\mathbf{r}}$ are given by equation (10) in Fig. 5 and converge to $\ddot{\mathbf{q}}$ and $\dot{\mathbf{q}}$. Fig. 5 shows the overall control system in block diagram form.

C. Engineering Tests

A preliminary evaluation of the system was preformed by observing the effect of shared control on the robot's trajectory near obstacles. In the first test, the robot was commanded to move the gripper in a straight line over a horizontal surface such that, without shared control, it would collide with a rectangular obstacle resting on the surface [see Fig. 7(a)]. In the second test, a master control was used to manually generate the commanded trajectory. In this test, the task was to approach a coffee mug

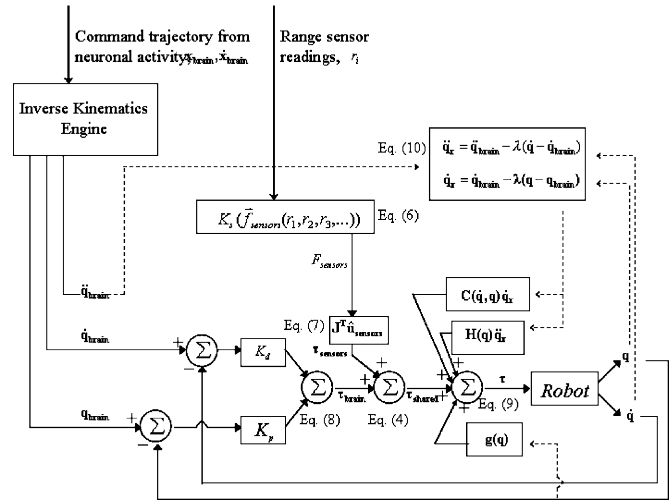

Fig. 5. Block diagram of the control system for the proposed CSC paradigm. Inputs are the Cartesian coordinates extracted from the brain signals and the range information from the sensors.

laying on its side (which served as the obstacle), move up and over the mug parallel to its curved side without touching it, and then come to rest with the gripper fingers on either side of the handle. The gripper collided with the cup and did not come to rest properly on the handle when the commanded trajectory selected for the test was generated [see Fig. 7(b)]. Note that while the rest of the system was the same as in the grasping task, a different gripper was used than the one shown in Fig. 3. The gripper used in the engineering tests was smaller and it had permanently open fixed-fingers. Also, the robot used in the engineering tests was a small workspace Phantom 1.5 (Sensable Technologies, Woburn, MA) as opposed to the large workspace Phantom 3.0 that was used in the grasping task.

D. Grasping Task

To evaluate the usefulness of shared control for BMI, the system was next tested on previously recorded brain-commanded trajectories to reach and grasp real objects. The neural data used were recorded from multiple cortical areas (M1, PMd, SMA, and S1) of the monkey [35], performing a reaching and grasping task with graphical feedback of targets and robot end position. In this original study, a robot (MANUS, Exact Dynamics, The Netherlands) was included in the loop, but the monkeys did not view it directly. Instead the monkeys viewed a computer monitor that displayed the location of the target object as a colored circle, and the location of the robot hand as another circle of different color. The monkey was trained to move the cursor to the target, and to modulate its grip force (indicated by cursor size) to achieve a target level of force (indicated as a ring around the target). The trial was considered successful if the monkey held the center of the cursor within the target for more than 150 ms, with the appropriate grasping force. The monkey could modulate the force prior to moving to the target. To make the slave robot's task analogous to the graphical task for which the monkeys were trained, a foam block was permanently mounted in the robot's gripper. This made the monkeys' task in online trials one of moving the

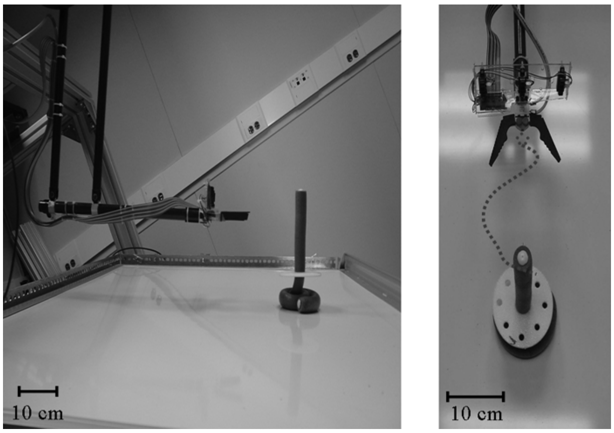

Fig. 6. Workspace reproduced offline with a robot (SensAble Technologies, Phantom 3.0), a target object, infrared proximity sensors and a pneumatic gripper. The dimensions of the workspace and target object are in proportion to those presented to the monkey on a computer screen during online trials. The dashed blue line shows a sample of a trajectory toward a target from a starting position marked by "o".

slave robot to the target location while squeezing with the target force. There was no object placed at the target location and, hence, the difficulties of inadvertently knocking the object away, or closing the gripper prematurely were not part of the online task. Also, the robot used for the original neural control trials was not equipped with CSC. The details of the online task have been reported previously [2].

In the online trials the monkey's hand position and grip force were recorded, as well as the activity of 183 neurons. Ten minutes of measured position and force data were used to train a linear model that approximated the mapping from neuronal activity to hand position and grip force. Once the model was trained, the cursor position and size of the cursor displayed for the monkey were determined solely by neuronal activity.

In the current study, the previously recorded data of Carmena *et al.* [2] were used in offline experiments on reaching and grasping of real objects. The predicted end point positions and grip forces, along with the position of the target objects were reproduced in a real workspace with a robot capable of CSC (Fig. 6). Relative sizes of the target object, workspace, gripper, and robot movement were consistent with the graphical game presented to the monkey when the neural data were recorded in the study of Carmena *et al.*. In contrast to the online experiments, however, the current experiments included real-world complexities such as prematurely closing the gripper and knocking the target object away. Also, to allow for the fact that the robot used in the offline tests did not have an articulated wrist, target locations were transformed so that the target object was always directly in front of the robot at the start of each trial.

The scale of the real workspace was chosen so that the real object was successfully situated within the gripper's span at times when the graphical cursor had been successfully inside the graphical target. The origin of the real workspace was chosen so that the gripper's sweet spot (shown in Fig. 3) centered on the real object at times when the graphical cursor had been centered on the graphical target. A total of 83 trials of the brain-controlled reach and grasp task were examined. For these trials, all cursor movement was controlled solely by neural signals without pole movement. In the online graphical game of Carmena *et al.*, all 83 trials were counted as successes.

In the offline setup, a trial was counted as successful if the gripper successfully grasped the object without knocking it over. The percentage of successful trials was recorded with CSC, with the contribution of the sensor commands weighted at 0%, 7%, 15%, 30%, and 48% of the weight of brain-derived commands. The percentage weight was determined by comparing the stiffness of the sensor response (Fig. 5, K_s) with stiffness of proportional controller (Fig. 5, K_p). To facilitate comparison, the Jacobian of the robot was used to map both stiffnesses into Cartesian space at the target location, where they could be expressed as (N/m) in the axial direction (Fig. 3, $\hat{\mathbf{u}}_{\mathbf{sensors}}$). In results comparing sensor-based weighting to brain-based weighting, the unitless ratio of these stiffnesses (N/m)/(N/m) is reported. The stiffness of the controller (K_p) was initially tuned prior to the trials to give optimal position control and subsequently remained constant throughout the trials. The stiffness of the sensor response (K_s) was changed during the trials to produce the reported weights for the sensor commands.

In the prior study of Carmena *et al.* [2], the size of the graphical cursor was determined solely by brain signals. In the present study, the grasping force of the gripper was determined solely by brain signals when the sensor-based commands were weighted 0%. However, in the CSC mode, when sensor-based commands were weighted 7%–48%, the proximity of the target cued the gripper activation.

III. Results

A. Engineering Tests

In engineering tests, these two reflexes were found to modify the commanded trajectory in several useful ways. Withdrawal commanded by the exterior sensors caused the gripper to avoid collisions of the outer gripper surfaces with objects in the scene. When the gripper approached large objects from the side, one of the outer two repulsive sensors detected the object first. This caused reflex withdrawal that tended to lift the gripper above it. Such reactions occurred when the exterior of the gripper was about to collide with the edge of a block [Fig. 7(a)]. When the gripper was situated above an object large enough to be detected by all three sensors, the central attractive sensor achieved an equilibrium with outer repulsive sensors. This led the gripper to hover conveniently over both flat surfaces, such as the top of a block [Fig. 7(a)] and gently curved surfaces such as the exterior of a coffee mug [Fig. 7(c)], despite a command trajectory that would have caused collisions [Fig. 7(b)]. However, objects or protuberances small enough to grasp, such as a coffee mug handle [Fig. 7(b) and (c)], tended to selectively activate the central sensor, attracting the gripper and biasing it toward closure.

B. Grasping Tasks

The number of successful trials initially increased with increased weighting of the sensor-derived commands. With CSC off (0% weight), 22 of the 83 trials were successful. Increasing the weight of sensor-derived commands to 7%, 15%, and 30%

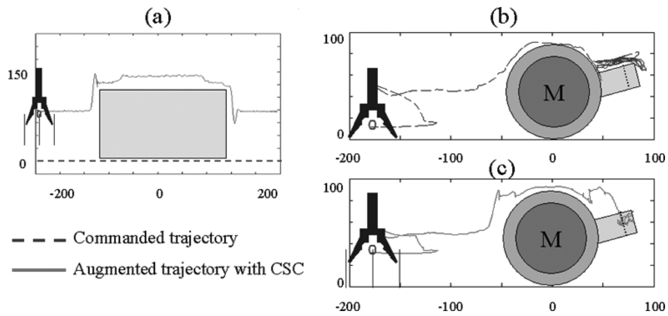

Fig. 7. Robot behavior augmented with CSC. The original trajectories are commanded by a human user. (a) The robot is able to hover above a planar surface and avoid collision with obstacles. (b) A raw noisy trajectory attempting to locate the handle of a coffee mug (marked "M") and the corresponding augmented trajectory (c). In (b) the robot collides with the surface of the mug and fails to locate the exact position of the handle. With sensor-based reflexes turned on, (c), the robot avoids collision, successfully hovers over the curved surface and locates the handle successfully.

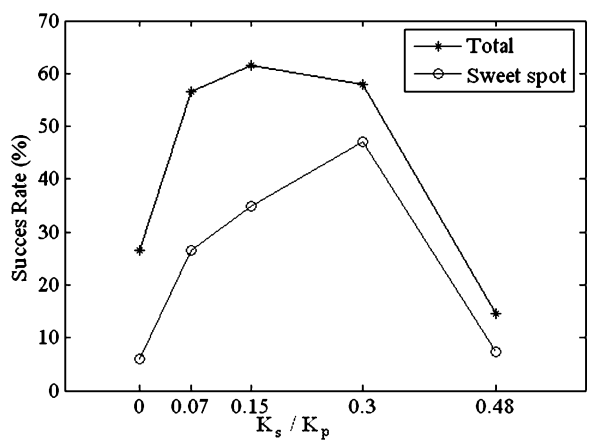

Fig. 8. Percentage success rate for the reproduced BMI trials.

of the brain-derived signals increased success to 47, 51, and 48 trials, respectively (Fig. 8). With the gain of sensor commands turned up to 48%, the number of successful trials dropped dramatically back down to 12, because the strong attraction of the gripper tended to knock the target object over. The number of successful trials that resulted in the object being grasped in the sweet spot of the gripper was also plotted (Fig. 8), showing a success rate of 6%, 27%, 35%, 46%, and 7% (5, 22, 29, 39, and 6 trials) with increasing weight of sensor command. Note that the sweet spot was the best location to hold the target object in order to maintain grip and orientation.

A typical trial with varying levels of CSC is shown (Fig. 9). Without CSC [Fig. 9(a)] the trial was a failure. Moderate CSC [Fig. 9(b)] led to a successful grasp, but not in the sweet spot. Further increase in gain [Fig. 9(c)] secured the target in the sweet spot. The highest gain [Fig. 9(d)] knocked the target away.

IV. Discussion

As reported in Carmena *et al.* [2], monkeys were able to use brain signals to successfully squeeze an object with the required force at the right location during online trials. The object was attached to the gripper and shown to the monkey as a virtual object on the computer screen. In the offline task reported in this paper,

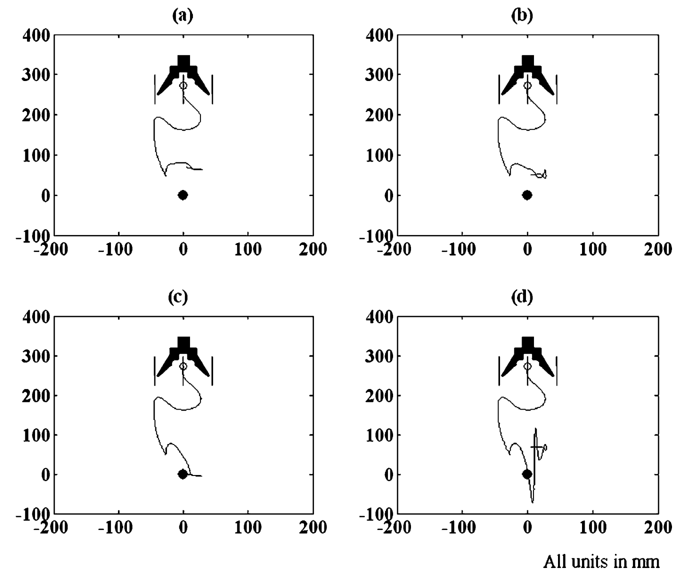

Fig. 9. Sample trajectory of the robot gripper with various levels of sensor-based control added. Coordinates of the target object (black circle) are indicated, as well as the initial coordinates of the gripper sweet spot "o", and the positions of the infrared proximity sensors (3 vertical lines): (a) 0% CSC; (b) 15% CSC; (c) 30% CSC; (d) 48% CSC.

the gripper needed to grasp an object positioned in the target location instead. This introduced difficulties such as knocking the target object away, or closing the gripper prematurely. These additional difficulties meant that only 27% of the trials counted as successful in the online computer game produced successful real-world grasps. This relatively low success rate reflects the fact that the monkey only received visual feedback related to an online computer game, not the real-world telerobotic grasping task, which was more difficult.

The grasping success rate was increased dramatically (Fig. 8) by the addition of sensors and CSC. Adding an optimal level of sensor-based reflex action increased the number of successful grasps by 2.3-fold. It also increased the number of grasps that secured the target object in the gripper "sweet-spot" by 7.7-fold.

The rise and fall in task performance with progressively increasing weighting of the sensor-based reflexes was a satisfyingly biomimetic result. Just as the human body can have too little reflex activity (hyporeflexive flacidity) or too much (hyperreflexive tremor), so could the robot have too little or too much reflex activity produced by its sensors. The best task performance occurred when brain-based commands were weighted 70%–85%, and sensor based reflexes were weighted 15%–30% (Fig. 8). It will be interesting to see whether this weighting produces optimal results in online trials as well.

The success rate of the trials may not be the only factor in choosing the ideal control weight for the sensors. As the weight of sensor-based commands is increased, the sensor-based components of the trajectories may eventually obscure the user's intention. As shown, (Fig. 10), the monkey's intended trajectory becomes less and less clear, as the attraction to the target becomes predominant. This may not be a problem in this simple reaching and grasping task, especially since there is only one target and the user can still withdraw from the target by pulling away in order to overcome the gripper's attraction to a graspable object. However, for more complicated tasks in more cluttered

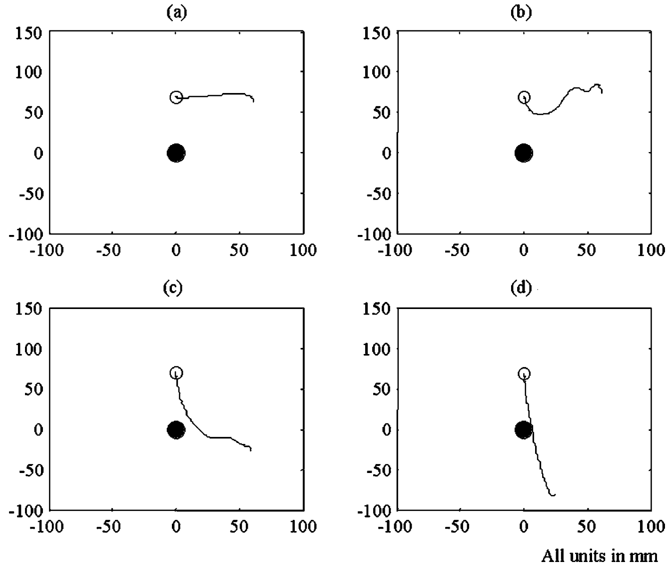

Fig. 10. A segment of the robot trajectory. This segment of the trajectory was chosen because the user's original intention was to move away from the target and shows one possible drawback of shared control. Coordinates of the target object (black circle) are indicated, as well as the initial coordinates of the gripper sweet spot "o", and the positions of the infrared proximity sensors (3 vertical lines). As the weight of the sensor-based reflexes is increased the trajectory becomes increasingly different from that derived purely from brain signals (upper left trajectory, 0% CSC); (a) 0% CSC; (b) 15% CSC; (c) 30% CSC; (d) 48% CSC.

environments excessively high sensor weights might cause the user to lose control of the robot.

The question of how much autonomy is ideal in BMI systems is an interesting one. Similar questions have been raised in telerobotic systems in the past. In teleoperation, total control can be given to the operator in a direct bilateral control system [36], [37]. At the other extreme, the robot can run autonomously in a hierarchical supervisory control framework where the operator only provides higher-level commands [38]. Also, there are various degrees of shared control that represent the middle ground, examples of which were given in the introduction. The level of autonomy given to the robot in teleoperation generally depends on the task, the environment, and the time delays involved in the system. Usually, if the tasks are well defined, performed in a known environment, involve a small number of motion primitives, and/or involve long time delays, more autonomy is given to the robot. If the task is performed in an unpredictable environment where the movement of the robot must be immediately responsive to the user's input and decisions have to be made instantaneously, the operator is given more direct control of the robot. Similar criteria would apply to use of shared control in BMI's.

Yet, there is an added dimension to the application of shared control to BMI. During brain control, the cortex has a limited communication bandwidth for commanding the robot, determined by the number of neurons that are being recorded. Carmena *et al.*, [2] showed that there is plastic cortical reorganization when the monkeys switch from operation with the hand to brain control. Primates appeared to optimize neural activity in order to control the robot/cursor through the limited communication channel provided by the recorded neuronal signal. Thus, it seems reasonable to ask what level of robot autonomy would provide for optimal cortical reorganization and robot control. Would a little robot autonomy lessen the computational load on the user's neuronal network, thus facilitating robot control? Might too much autonomy lead to poor correlations of the robot trajectory with the user's natural arm movements, hindering cortical reorganization and robot control? The question of how the cortex responds to different levels of robot autonomy is an interesting direction for future studies. Graded levels of robot autonomy might also facilitate training users in BMI control. For example, the training of a paralyzed human user, or a nonhuman primate, could start with pure supervisory control. As cortical control of the robot is mastered, one might slowly decrease the level of robot autonomy, allowing the user's cortical plasticity to gradually subsume low-level flexible control of the manipulator.

A potential drawback of shared control is that flexibility of the system may be lost. It is worth noting that the type of partial autonomy given to the robot in this study would not have made any of the points in a workspace unreachable to a human or nonhuman primate user. Because control was shared, every point in the space remained reachable to a user capable of modulating motor commands well enough to offset the contribution of the sensors. In principle, objects could still be "almost but not quite" touched, if that were the user's goal. Likewise, a user could have pushed around an object with the outer edges of the gripper by adjusting his or her motor command to offset the sensor-based withdrawal reflex.

Also, it is important to acknowledge one of the main shortcomings of the results described in this paper. As described previously, CSC has been demonstrated here using prerecorded neural data. The offline nature of this demonstration omits the important effects of visual feedback to the brain. Given feedback, the brain would have a chance to adapt and learn the new dynamics introduced by shared control, potentially producing different results from those reported here. Despite this limitation, the results show unambiguously that CSC improved task success significantly, even without online adaptation and learning of the brain. It seems reasonable to suppose that online visual feedback to the monkey of the resulting robot trajectories might lead to further enhancements in performance. However, whether CSC improves or diminishes performance during on-line trials has yet to be shown and is a subject for further studies.

The design space of BMI shared control systems appears to be large, and rich with interesting possibilities. For example, the shared control paradigm provides a convenient framework for incorporating the software equivalent of a central pattern generator into a walking BMI. A more pedestrian improvement to shared control BMI's would be to put the weight of the sensor-derived commands under the user's instantaneous brain control. Activity of cortical neurons is well known to reflect focused attention [6], [39]–[41]. Therefore, monitoring user's spatial attention and analyzing the corresponding neuronal patterns may provide the key to adjusting sensor-derived commands on the fly. It also looks feasible to make the type of reflex response that the sensors generate (attraction, repulsion) subject to the user's continuous control. Furthermore, it would be interesting to replace the practical, linear, attractive/repulsive reflex actions used in this study with time-varying reflexes designed to mimic spinal reflexes as closely as possible. This would facilitate quantitative comparisons between the optimal weighting of robot reflexes and the optimal weighting of spinal reflexes compared to the user's central motor drive. In future applications the type of control, ranging from purely supervisory to purely reflexive, might be determined postsurgery, based on the type of information that the subsample of recorded neurons best represents. If neurons representing higher-level information such as task goals and target objects were mainly acquired, the robot could operate close to supervisory control, whereas if neurons carrying lower-level trajectory information were acquired, the cortex could be given more direct control.

It has been the authors' intention to introduce a general purpose CSC paradigm for brain machine interfaces. The specific problem of grasping in unstructured environments, and the specific implementation of the gripper, range sensors, and reflex actions were intended primarily to illustrate the approach. It seems clear the present study has only scratched the surface of what sensor based actions and increased autonomy could add to the capabilities of BMI's. Regardless of the specific implementation, the paradigm of CSC can provide a framework for adding more complex and interesting BMI components in the future.

REFERENCES

[1] J. Wessberg, C. R. Stambaugh, J. D. Kralik, M. Laubach, J. K. Chapin, J. Kim, S. J. Biggs, M. A. Srinivasan, and M. A. L. Nicolelis, "Real-time prediction of hand trajectory by ensemble of cortical neurons in primates," *Nature*, vol. 408, pp. 361–365, 2000.

[2] J. M. Carmena, M. A. Lebedev, R. E. Crist, J. E. O'Doherty, D. M. Santucci, D. Dimitrov, P. G. Patil, C. S. Henriquez, and M. A. L. Nicolelis, "Learning to control brain-machine interface for reaching and grasping by primates," *PloS Biol.*, vol. 1, pp. 192–203, 2003.

[3] M. D. Serruya, N. G. Hatsopoulos, L. Paninski, M. R. Fellows, and J. P. Donoghue, "Instant neural control of a movement signal," *Nature*, vol. 416, pp. 141–142, 2002.

[4] D. M. Taylor, S. I. Tillery, and A. B. Schwartz, "Direct cortical control of 3D neuroprosthetic devices," *Science*, vol. 296, pp. 1829–1832, 2002.

[5] L. Shen and G. E. Alexander, "Preferential representation of instructed target location versus limb trajectory in dorsal premotor area," *J. Neurophysiol.*, vol. 77, no. 3, pp. 1195–1212, 1997.

[6] M. A. Lebedev and S. P. Wise, "Tuning for the orientation of spatial attention in dorsal premotor cortex," *Eur. J. Neurosci.*, vol. 13, no. 5, pp. 1002–1008, 2001.

[7] D. J. Crammond and J. F. Kalaska, "Modulation of preparatory neuronal activity in dorsal premotor cortex due to stimulus-response compatibility," *J. Neurophysiol.*, vol. 71, no. 3, pp. 1281–1284, 1994.

[8] L. A. Jones, "Dexterous hands: human, prosthetic and robotic," *Presence*, vol. 6, pp. 29–56, 1997.

[9] B. Hannaford, L. Wood, D. A. McAffee, and H. Zak, "Stability and performance tradeoffs in bi-lateral telemanipulation," *IEEE Trans. Syst. Man Cybern.*, vol. 21, no. 3, pp. 1764–1767, 1991.

[10] M. Massimino and T. B. Sheridan, "Teleoperator performance with varying force and visual feedback," *Hum. Factors*, vol. 36, no. 1, pp. 145–157, 1994.

[11] S. G. Meek, S. C. Jacobsen, and P. P. Goulding, "Extended physiological taction: design and evaluation of a proportional force feedback system," *J. Rehabil. Res. Dev.*, vol. 26, pp. 53–62, 1989.

[12] M. Burstedt, B. Edin, and R. Johansson, "Coordination of fingertip force during human manipulation can emerge from independent neural networks controlling each engaged digit," *Exp. Brain Res.*, vol. 117, pp. 67–79, 1997.

[13] K. Salisbury, "Issues in human/computer control of dexterous remote hands," *IEEE Trans. Aerosp. Electron. Syst.*, vol. 24, pp. 591–596, 1988.

[14] S. Hayati and S. T. Venkataraman, "Design and implementation of a robot control system with traded and shared control capability," in *Proc. IEEE Int. Conf. Robotics and Automation*, 1989, vol. 3, pp. 1310–1315.

[15] S. P. Levine, D. A. Bell, L. A. Jaros, R. C. Simpson, Y. Koren, and J. Borenstein, "The NavChair assistive wheelchair navigation system," *IEEE Trans. Rehab. Eng.*, vol. 7, no. 4, pp. 443–451, Dec. 1999.

[16] G. Wasson, J. Gunderson, S. Graves, and R. Felder, "Effective shared control in cooperative mobility aids," in *FLAIRS 2001*, pp. 509–513.

[17] M. Oda, N. Inaba, Y. Takano, S. Nishida, M. Kayashi, and Y. Sugano, "Onboard local compensation on ETS-W space robot teleoperation," in *Proc. IEEE/ASME Int. Conf. Advanced Intelligent Mechatronics*, 1999, pp. 701–706.

[18] P. G. Backes, "Multi-sensor based impedance control for task execution," in *Proc. IEEE Int. Conf. Robotics and Automation*, 1992, vol. 2, pp. 1245–1250.

[19] P. Michelman and P. Allen, "Shared autonomy in a robot hand teleoperation system," in *Proc. IEEE/RSJ/GI Int. Conf. Intelligent Robots and Systems*, 1994, vol. 1, pp. 253–259.

[20] L. Li, B. Cox, M. Diftler, S. Shelton, and B. Rogers, "Development of a telepresence controlled ambidextrous robot for space applications," in *Proc. IEEE Int. Conf. Robotics and Automation*, 1996, vol. 1, pp. 58–63.

[21] L. Turki and P. Coiffet, "On grasp synthesis and planning of multifingered robot hands for a telemanipulation task," in *Proc. IEEE Int. Workshop on Robot and Human Communication*, 1995, pp. 141–146.

[22] B. Brunner, K. Arbter, and G. Herzinger, "Task directed programming of sensor based robots," in *Proc. IEEE/RSJ/GI Int. Conf. Intelligent Robots and Systems*, 1994, vol. 2, pp. 1080–1087.

[23] C. S. Lovchik and M. A. Diftler, "The Robonaut hand: a dexterous robot hand for space," in *Proc. IEEE Int. Conf. Robotics and Automation*, 1999, vol. 2, pp. 907–912.

[24] R. O. Ambrose, H. Aldridge, R. S. Askew, R. R. Burridge, W. Bluethmann, M. Ditfler, C. Lovchick, D. Magruder, and F. Rehnmark, "Robonaut: NASA's space humanoid," *IEEE Intell. Syst. Applicat. Mag.*, vol. 15, no. 4, pp. 57–62, Jul.–Aug. 2000.

[25] W. B. Griffin, "Shared Control for Dexterous Telemanipulation," Ph.D. dissertation, Dept. of Mech. Eng., Stanford Univ., Stanford, CA, 2003.

[26] R. A. Brooks, "A robust layered control system for a mobile robot," *IEEE J. Robotic. Autom.*, vol. 2, no. 1, pp. 14–23, 1986.

[27] A. Matsikis, M. Schmitt, M. Rous, and K. F. Kraiss, "Ein Konzept für die mobile Manipulation von unbekannten Objektenmit Hilfe von 3D-Rekonstruktion und Visual Servoing," *Informatik Aktuell, Fachgespräch AMS*, vol. 15, pp. 179–187, Nov. 1999.

[28] B. K. Horn, *Robot Vision*. Cambridge, MA: MIT Press, 1986.

[29] S. Hutchinson, G. Hager, and P. Corke, "A tutorial on visual servo control," *IEEE Trans. Robot. Autom.*, vol. 12, no. 5, pp. 651–670, Oct. 1996.

[30] D. Kragic and H. Christensen, "Robust visual servoing," *Int. J. Robot. Res. (Special Issue on Visual Servoing)*, vol. 22, no. 10–11, pp. 923–940, Oct. 2003.

[31] O. Khatib, "Real-time obstacle avoidance for manipulators and mobile robots," *Int. J. Robot. Res.*, vol. 5, no. 1, pp. 90–98, 1986.

[32] J.-J. E. Slotine and W. Li, *Applied Nonlinear Control*. Englewood Cliffs, NJ: Prentice-Hall, 1991.

[33] A. Levinsson, M. Garwicz, and J. Schouenborg, "Sensorimotor transformation in cat nociceptive withdrawal reflex system," *Eur. J. Neurosci.*, vol. 11, pp. 4327–4332, 1999.

[34] D. I. Zafeiriou, I. G. Tsikoulas, and G. M. Kremenopoulos, "Prospective follow-up of primitive reflex profiles in high-risk infants: clues to early diagnosis of cerebral palsy," *Pediatr. Neurol.*, vol. 13, no. 2, pp. 148–152, 1995.

[35] M. A. L. Nicolelis, D. Dimitrov, J. M. Carmena, R. E. Crist, G. Lehew, J. Kralik, and S. Wise, "Chronic, multi site, multi electrode recordings in macaque monkeys," *Proc. Nat. Acad. Sci.*, vol. 100, no. 19, pp. 11 041–11 046, 2003.

[36] D. A. Lawrence, "Stability and transparency in bilateral teleoperation," *IEEE Trans. Robot. Autom.*, vol. 9, no. 5, pp. 624–637, Oct. 1993.

[37] Y. Yokokohji and T. Yoshikawa, "Bilateral control of master-slave manipulators for ideal kinesthetic coupling-formulation and experiment," *IEEE Trans. Robot. Autom.*, vol. 10, no. 5, pp. 605–620, Oct. 1994.

[38] T. B. Sheridan, *Telerobotics, Automation, and Human Supervisory Control*. Cambridge, MA: MIT Press, 1992.

[39] J. H. Reynolds, L. Chelazzi, and R. Desimone, "Competitive mechanisms subserve attention in macaque areas V2 and V4," *J. Neurosci.*, vol. 19, no. 5, pp. 1736–1753, Mar. 1999.

[40] S. Kastner and L. G. Ungerleider, "Mechanisms of visual attention in the human cortex," *Annu. Rev. Neurosci.*, vol. 23, pp. 315–341, 2000.

[41] C. L. Colby and M. E. Goldberg, "Space and attention in parietal cortex," *Annu. Rev. Neurosci.*, vol. 22, pp. 319–349, 1999.

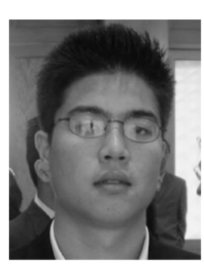

Hyun K. Kim received the S.B. and S.M. degrees in mechanical engineering from the Massachusetts Institute of Technology (MIT), Cambridge, in 2000 and 2002, respectively.

He is currently a research assistant at the MIT Touch Laboratory and a Ph. D. candidate at the Mechanical Engineering Department, MIT. His research interests include neural control of motion, brain-machine interfaces, robotics and virtual reality devices.

S. James Biggs (S'97–M'99) received the B.A. degree in human biology from Stanford University, Stanford, CA, in 1991, and the Ph.D. degree in bioengineering from the University of Utah, Salt Lake City, in 1999.

After a two-year Postdoc at the MIT Touch Laboratory, he became a Research Scientist within the MIT Research Laboratory of Electronics, Cambridge. He is the author of numerous articles on human touch and proprioception, and has three patents pending in the areas of tactile displays and neuroprosthetics.

David W. Schloerb received the S.B. degree in physics and the S.M. and Ph.D. degrees in mechanical engineering from the Massachusetts Institute of Technology (MIT), Cambridge, in 1977, 1982, and 1997, respectively.

He was employed for several years as a Mechanical Engineer doing work related to diving and hyperbaric systems. His projects at MIT have included: design and construction of an underwater welding system (US Patent #4 475 026), design and construction of an underwater robotic arm, development of a quantitative theory of telepresence, and psychophysical experiments on perceptual adaptation in virtual environments. He is currently a Postdoctoral Associate in the MIT Touch Laboratory with research interests ranging from presence theory, to experimental psychophysics, to hardware and software design.

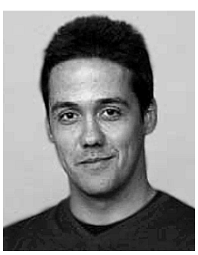

Jose M. Carmena (S'99–M'02) received the B.S. and M.S. degrees in electrical engineering from the Polytechnic University of Valencia, Valencia, Spain, in 1995 and the University of Valencia, Valencia, in 1997. He received the M.S. degree in artificial intelligence and the Ph.D. degree in robotics both from the University of Edinburgh, Edinburgh, U.K., in 1998 and 2002, respectively.

From 2002 to 2005 he was a Postdoctoral Fellow at Miguel Nicolelis' Laboratory, Department of Neurobiology, and the Center for Neuroengineering at Duke University, Durham, NC. He was appointed assistant professor in the Department of Electrical Engineering and Computer Sciences, and the Helen Wills Neuroscience Institute at the University of California, Berkeley, in the summer of 2005. His research interests include neural engineering (brain-machine interfaces; neuroprosthetics; biomimetic robotics), and systems and cognitive neuroscience (neural basis of sensorimotor control and learning; neural ensemble computation).

He was the recipient of a Christopher Reeve Paralysis Foundation research award. He is member of the IEEE RAS and EMBS societies, the Society for Neuroscience, and the Neural Control of Movement Society.

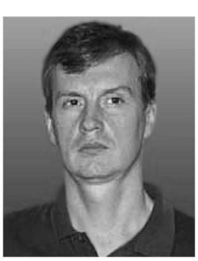

Mikhail A. Lebedev born in Moscow, Russia, on March 4, 1963. He received the M.Sci. degree in physics from the Moscow Institute of Physics and Technology, Moscow, 1986, and the Ph.D. degree in neurobiology from University of Tennessee, Memphis, in 1995.

He is currently a Senior Research Scientist at Duke University Center for Neuroengineering, Durham, NC. His research interests include neurobiology, and brain-machine interfaces.

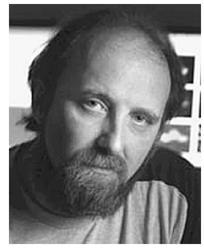

Miguel A. L. Nicolelis is a native of Sao Paulo, Brazil, and received the M.D. and Ph.D. degrees in neurophysiology from the University of Sao Paulo, Sao Paulo, in 1984 and 1988, respectively.

After postdoctoral work at Hahnemann University, he joined Duke University in 1994, where he is the Anne W. Deane Professor of Neuroscience, Co-Director of the Center for Neuroengineering, and Professor of Neurobiology, Biomedical Engineering, and Psychological and Brain Sciences. Neuroscience laboratories in the US and Europe have incorporated Dr. Nicolelis' experimental paradigm to study a variety of mammalian neuronal systems. His research has influenced basic and applied research in computer science, robotics, and biomedical engineering. This multidisciplinary approach to research has become widely recognized in the neuroscience community. He is interested in understanding the general computational principles underlying the dynamic interactions between populations of cortical and subcortical neurons involved in motor control and tactile perception. He has authored more than 100 manuscripts in scientific journals and edited 6 books and special journal issues, and has been an invited speaker at numerous scientific conferences and meetings throughout the world.

As a student, Dr. Nicolelis was awarded the Oswaldo Cruz Prize for research, the highest honor awarded to a Brazilian medical student. He has received numerous honors and awards including the Whitehead Scholar Award in 1994; 2002 DARPA Award for Sustained Excellence by a Performer; the 2002 Ruth and A Morris Williams, Jr. Faculty Research Prize; Whitehall Foundation Award; McDonnell-Pew Foundation Award; 2003 Duke University Thomas Langford Lectureship Award; 2004 Grass Traveling Scientist Program Distinguished Lecturer UCLA; 2004 Ramon y Cajal Chair, University of Mexico, Mexico City; and 2005 Santiago Grisolia Chair, Catedra Santiago Grisolia.

Mandayam A. Srinivasan received the Bachelors degree in civil engineering from Bangalore University, Bangalore, India, the Masters degree in aeronautical engineering from the Indian Institute of Science, Bangalore, and the Ph.D. degree in applied mechanics from Yale University, New Haven, CT.

He worked as a member of the research staff at the Department of Anesthesiology, Yale University School of Medicine, where he conducted research on the mechanics and mechanisms of the primate sense of touch. Since 1987, he has been at the Massachusetts Institute of Technology (MIT), Cambridge, where he founded the Laboratory for Human and Machine Haptics, informally known as the Touch Lab (http://touchlab.mit.edu). He is currently the Director of the Touch Lab and a Senior Research Scientist with the Department of Mechanical Engineering and the Research Laboratory of Electronics at MIT. His research on the science and technology underlying information acquisition and object manipulation through touch has fundamentally contributed to the emergence of the new and exciting field of Haptics. He has been recognized worldwide as an authority on haptic computation, cognition, and communication in humans and machines, particularly to enhance human-machine interactions in virtual environment systems. He has conducted pioneering investigations in skin biomechanics, tactile neuroscience, sensorimotor psychophysics, haptic device design and multimodal rendering algorithms, and has demonstrated novel applications of this multidisciplinary research in areas such as the development of multiuser haptics in shared virtual environments, medical simulations involving force feedback for training, and direct control of machines from brain neural signals. He has authored articles in leading journals in many fields and has been an invited speaker at numerous scientific conferences. His work has been featured in print, radio, and television media around the world in news articles and programs focused on cutting edge research in information technology and its future prospects.

Dr. Srinivasan has served as a member of the National Academy of Sciences committee on virtual reality and teleoperator systems, the MIT Virtual Environment and Teleoperation Research Consortium and the editorial board of the MIT Press journal PRESENCE: Teleoperators and Virtual Environments. He is also a member of the Society for Neuroscience.